SCIENCE OF THE TOTAL ENVIRONMENT 399 (2008) 147–157

available at www.sciencedirect.com

ScienceDirect

www.elsevier.com/locate/scitotenv

Process analysis of typical summertime ozone episodes over the Beijing area

Jun Xu[a,*], *Yuanhang Zhang*[b], *Joshua S. Fu*[c], *Shaoqing Zheng*[d], *Wei Wang*[a]

[a]*Chinese Research Academy of Environmental Sciences, Beijing, 100012, China*
[b]*College of Environmental Sciences, Peking University, Beijing, 100871, China*
[c]*Department of Civil and Environmental Engineering, The University of Tennessee, Knoxville, Tennessee, 37996, USA*
[d]*Appraisal Center For Environment & Engineering, State Environmental Protection Administration, Beijing, 100012, China*

ARTICLE INFO

Article history:
Received 26 June 2007
Received in revised form
1 February 2008
Accepted 4 February 2008
Available online 2 May 2008

Keywords:
Ozone
Air quality model
Process analysis
Beijing
Urban downwind area

ABSTRACT

The 2008 Summer Olympic Games will be held in Beijing; however, summer is the season in which Beijing is marked by frequent high-O_3 episodes. Observation analysis reveals that the urban plume is transported by a southerly wind and undergoes chemical reaction during propagation, resulting in the common occurrence of high O_3 concentrations in the urban downwind area; this is the typical scenario of the formation of high summertime O_3 levels over the Beijing area. The typical high-O_3 episode is well reproduced by the 3-dimensional air-quality model CMAQ-MADRID (Community Multi-scale Air-Quality Model of Aerosol Dynamics, Reaction, Ionization, and Dissolution). Radical cycle analysis reveals that the Beijing urban area was in a VOC-limited regime for O_3 formation, while the urban downwind area changed gradually to a NO_x-limited condition. The urban downwind area, Dingling, is readily affected by intrusion of the urban plume. Detailed process analysis indicated that although the O_3 peaks reached the same level on 26 and 27 June 2000, the dominant process contributing to the O_3 increase was different on each day. On 26 June, the major contributor to the O_3 peak at Dingling was the arrival of high O_3 levels with propagation of the urban plume; in contrast, on 27 June O_3 precursors were transported rapidly to the urban downwind area by strong transportation processes that occurred earlier than those on the previous day, resulting in O_3 production by local photochemistry becoming the major contributor to the high-O_3 episode.

1. Introduction

Vigorous economic development and rapid urbanization have led to increased emissions of various pollutants from urban areas in China, making high-O_3 episodes one of the most severe problems in terms of urban air pollution (Zhang et al., 1998; Shao et al., 2006). The formation of O_3 is a complex process, involving various chemical and physical mechanisms. Numerical modeling establishes a link between emissions and ambient concentrations based on assumed physical and chemical processes, thereby providing a useful tool in performing detailed process analyses of O_3 formation. Most simulation studies employ models as a 'black box' (Jeffries and Tonnesen, 1994), using the model to simulate the temporal and spatial distribution of O_3 or other pollutants and then compare predicted and observed data (Steve et al., 2006; Zhang et al., 2006). Other studies have assessed the sensitivity of O_3 formation to the emission of precursors by perturbing the

* *Corresponding author*. Tel.: +86 10 84915249; fax: +86 10 84915248.
E-mail address: xujun@craes.org.cn (J. Xu).

0048-9697/$ – see front matter © 2008 Elsevier B.V. All rights reserved.
doi:10.1016/j.scitotenv.2008.02.013

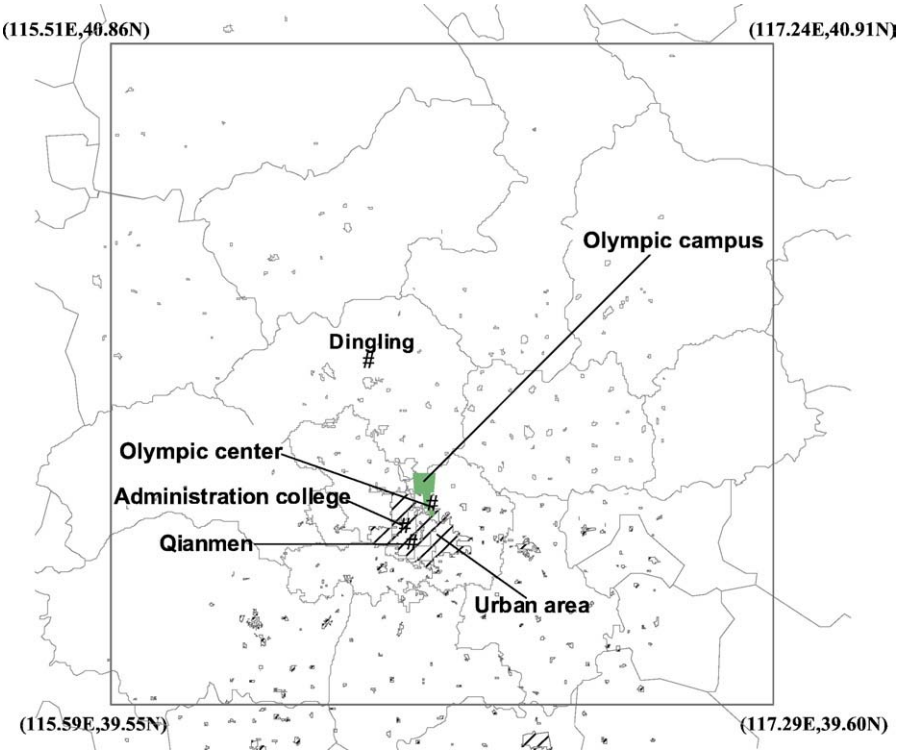

Fig. 1 – Innermost mesh of the simulation of the Beijing area, with an area of 144 × 144 km; the symbol # represents monitoring stations.

emission inventory (Streets et al., 2007; Wang and Li, 2003); however, few publications in English journals have explored the process analysis method of O_3 formation or identified the contribution of different physical and chemical processes in terms of the quantity of produced O_3 in CMAQ in Beijing area, though there are a few applications in Hong Kong and rural China (Huang et al., 2005; Wang et al., 2006).

A comprehensive summertime field campaign was conducted in the Beijing area from 21 June to 6 July 2000 (Wang, 2002), involving 12 automatic stations and 6 intensive stations located in urban, suburban, and extra-urban areas, thereby generating large datasets for further research. During the field campaign, high O_3 concentrations were recorded in the Beijing area, especially in the urban downwind area where peak levels exceeded 200 ppb. These high-O_3 events provide suitable cases for observation analysis and model simulations in exploring the processes governing typical summertime O_3 formation over the Beijing area.

In this work, we first perform an observation analysis to identify a typical summertime O_3 episode over the Beijing area. The 3-dimensional air-quality model CMAQ-MADRID is then employed to simulate and analyze the observed cases. The model domain for the Beijing area is shown in Fig. 1. IPR (Integrated Process Rate analysis) and IRR (Integrated Reaction Rate analysis; Jeffries and Tonnesen, 1994) equipped in CMAQ are useful tools in performing process analysis on the results of model simulations. Here, we use the tools to conduct a detailed process analysis of typical O_3 episodes in the Beijing area. This is undertaken to identify the dominant process contributing to O_3 formation and determine the characteristics of the photochemical system at different locations or at a given location on different days.

2. Observations

2.1. *Surface wind*

The Beijing urban area occupies flat terrain, but is bound by areas of complex topography, facing Yan Mountains to the north and Taihang Mountains to the west. The urban area is located 30–40 km from the mountain regions, with a contrast in elevation of about 500–1500 m (Climatology in Beijing, 1987; Li et al., 1982); thus, near-surface airflow is strongly influenced by terrain effects (Cai et al., 2002). In fact, the lower atmosphere over the Beijing area is controlled by the combined effects of the diurnal circulation of mountain-valley wind, the urban heat island effect, and the synoptic weather system, making for a complicated flow pattern (Xu et al., 2002). During the weak summertime synoptic situation, the surface wind direction and speed show diurnal variations, demonstrating the characteristics of the local mountain-plain circulation pattern, which is the typical lower airflow mode in the Beijing area during summer; i.e., the low-velocity down-valley northerly wind dominates the area at night, while the high-velocity up-valley southerly wind dominates the area during the daytime (Cai et al., 2002).

Fig. 2 shows the surface wind fields simulated by MM5 (Fifth-generation PSU/NCAR Mesoscale Model, Grell et al., 1994) with observed wind vectors from different stations

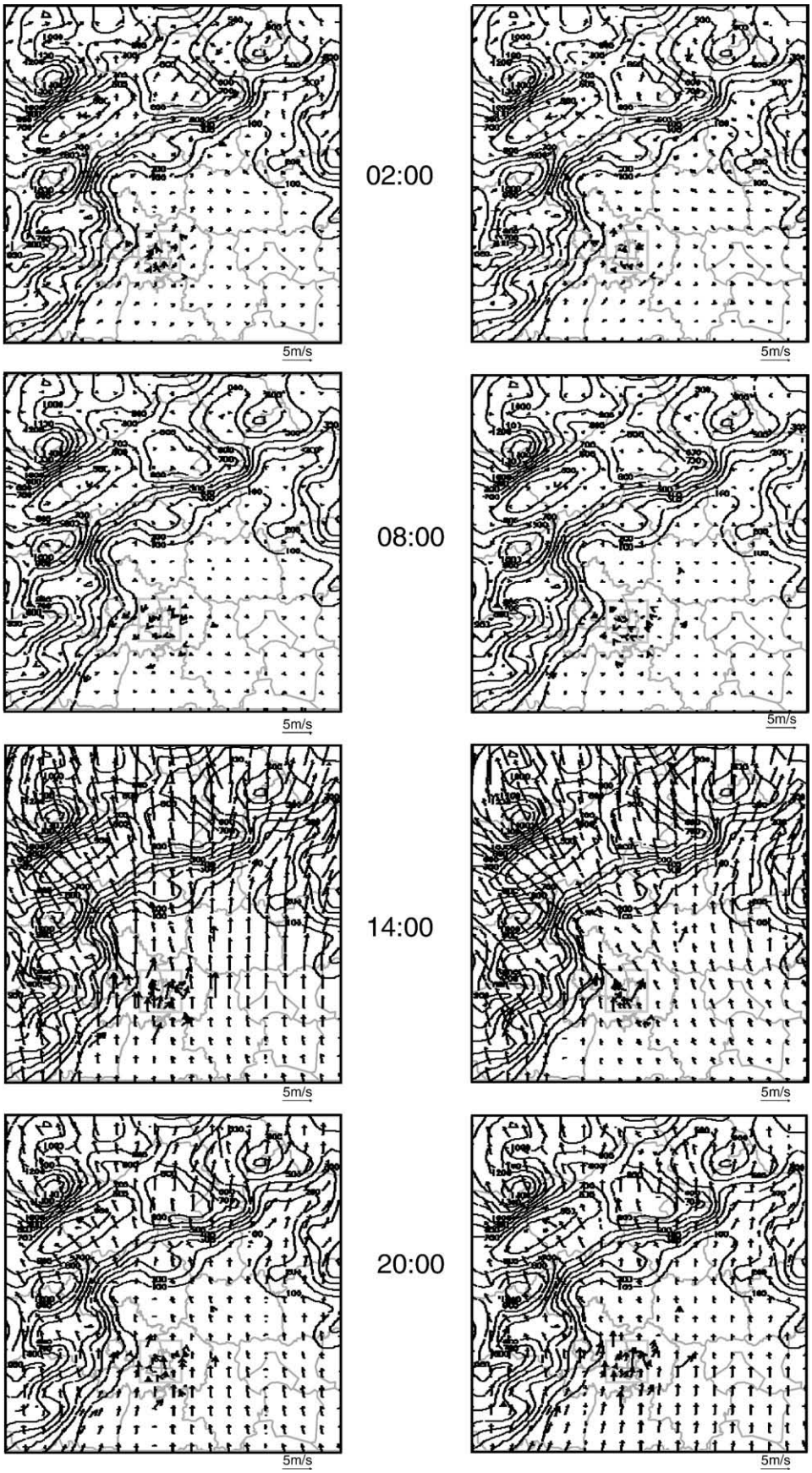

Fig. 2 – Diurnal variations of surface wind field simulated by MM5 with observed wind vectors from different stations overlapped during 26 June (left column) and 27 June (right column) 2000 in the Beijing area, thick arrows represent observed surface wind vectors, inner box delimited the urban area.

overlapped. Each figure represents a specific time over the period from 26 June to 27 June 2000, reflecting the diurnal variation in lower airflow patterns for the region. At 0200 LST on 26 June, the southerly wind was dominant across the region from the Beijing urban area north to Changping County, while wind field was not so much in order for the mountainous region in the northern part of the domain; wind speeds were relatively weak across the entire domain. At 0800 LST on 26 June, a northerly wind generated by the terrain effect controlled the area with flat terrain (covering the Beijing urban area), albeit with low velocities. The wind field experienced a transition during the morning hours, with calm conditions or light wind across the region. In the afternoon, a strong southerly wind began to dominate the entire domain, leading to a strong transportation effect that continued until 2000 LST on 26 June. On 27 June, the diurnal variation in wind fields was similar to that recorded on 26 June, although the change in the wind field began earlier than that in the previous day. The southerly wind extended to the urban area from 0800 LST, indicating that transportation upon the prevailing southerly wind began earlier on 27 June than on 26 June, with a stronger transportation effect. It can be concluded that the lower airflow mode exhibited a typical summertime diurnal circulation pattern in the Beijing area over the 2 days, and the simulated wind fields captured the characteristics. Given that Dingling is located downwind of the Beijing urban area upon southerly wind, it is readily affected by the urban plume.

2.2. *Monitoring of pollutants*

CO is relatively inactive in terms of photochemistry, and emissions from the Beijing urban area are much higher than those from the surrounding area (Wang, 2002). Consequently, CO concentrations can be viewed as tracers of transportation of the urban plume. As shown in Fig. 3a, the diurnal mode of variation in CO in the urban area differed from that in the downwind area of Dingling on both 26 and 27 June. The urban area was defined as the area inside the 4th ring road, which was delimited by the inner box as shown in Fig. 2. In this case, there are totally 8 sites belonging to the urban area. Thus, their CO average was treated as the urban value. In the urban area, CO peaks appeared in the morning, arising from elevated CO emissions and the incomplete development of the boundary layer. At Dingling, clear CO peaks appeared late in the afternoon, and peak concentrations occurred at times of transportation upon strong southerly winds, testifying to the fact that high pollutant concentrations at Dingling coincide with the arrival of the urban plume. In comparing diurnal CO variations at Dingling over the two days, the CO peak on 27 June was more pronounced than that on 26 June, and the peak value on this day was more similar to that of the urban area, indicating that the urban plume was transported more effectively to Dingling on 27 June.

On 26 and 27 June, the O_3 peak at Dingling occurred in the afternoon, when a strong southerly wind prevailed (Fig. 3b). The peak time occurred 2–3 h later than that in the urban area, and the peak values at Dingling were higher than those recorded in the urban area. Based on the above analysis of diurnal variations in the wind field and concentrations of pollutant, we conclude that the strongly polluted urban plume

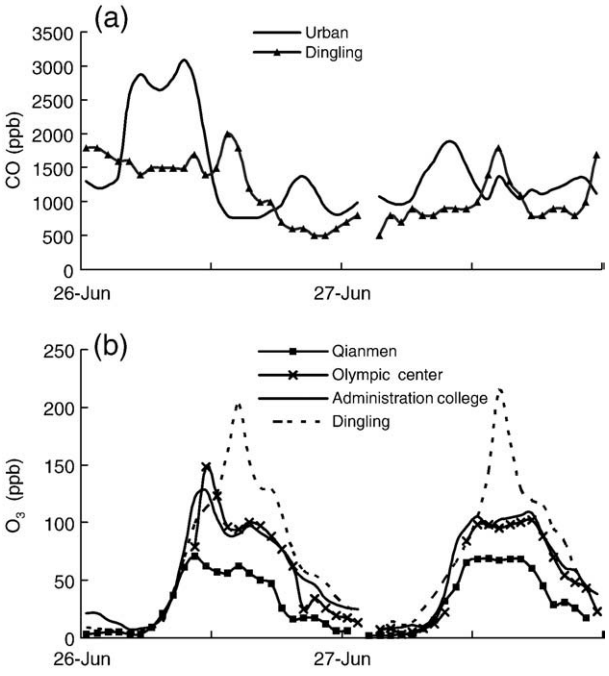

Fig. 3 – Diurnal variations in observed CO (a) and O_3 (b) at the urban area and the downwind area of Dingling from 26 June to 27 June 2000.

underwent photochemical reactions while moving within the prevailing southerly wind, resulting in gradually increasing O_3 concentrations with ongoing propagation of the plume. Such an evolution of pollutants is the typical summertime process of O_3 formation in the Beijing area. The above findings also indicate that the transportation of O_3 and its precursors from the urban area may contribute to the high O_3 concentrations recorded in the downwind urban area.

3. O_3 simulation

3.1. *Simulation description*

CMAQ-MADRID (Zhang et al., 2004) was employed for the simulation, using CMAQ (Byun and Ching, 1999) as a host model and adopting modules of the transportation processes provided in the original CMAQ (e.g., advection and turbulent diffusion), although with improvements to all modules concerned with aerosol processes. In our simulation, a two-section size representation, typically for fine and coarse particles, was selected to reduce computation time. CBIV (Carbon Bond mechanism, version IV; Gery et al., 1989) was selected as the gaseous chemical mechanism, including the four heterogeneous reactions suggested by Jacob (2000). ISORROPIA (Nenes et al., 1998) was used as the thermodynamic module for gas-particle partitioning.

A three-level nesting was used for the simulation. The domain for the first level covered all of East Asia. The second-level domain covered a large part of North China, including Hebei, Beijing, and Tianjin, and parts of the areas of Shanxi, Shandong, Liaoning, and Inner Mongolia. The third-level domain focused on the Beijing area (Fig. 1), including both

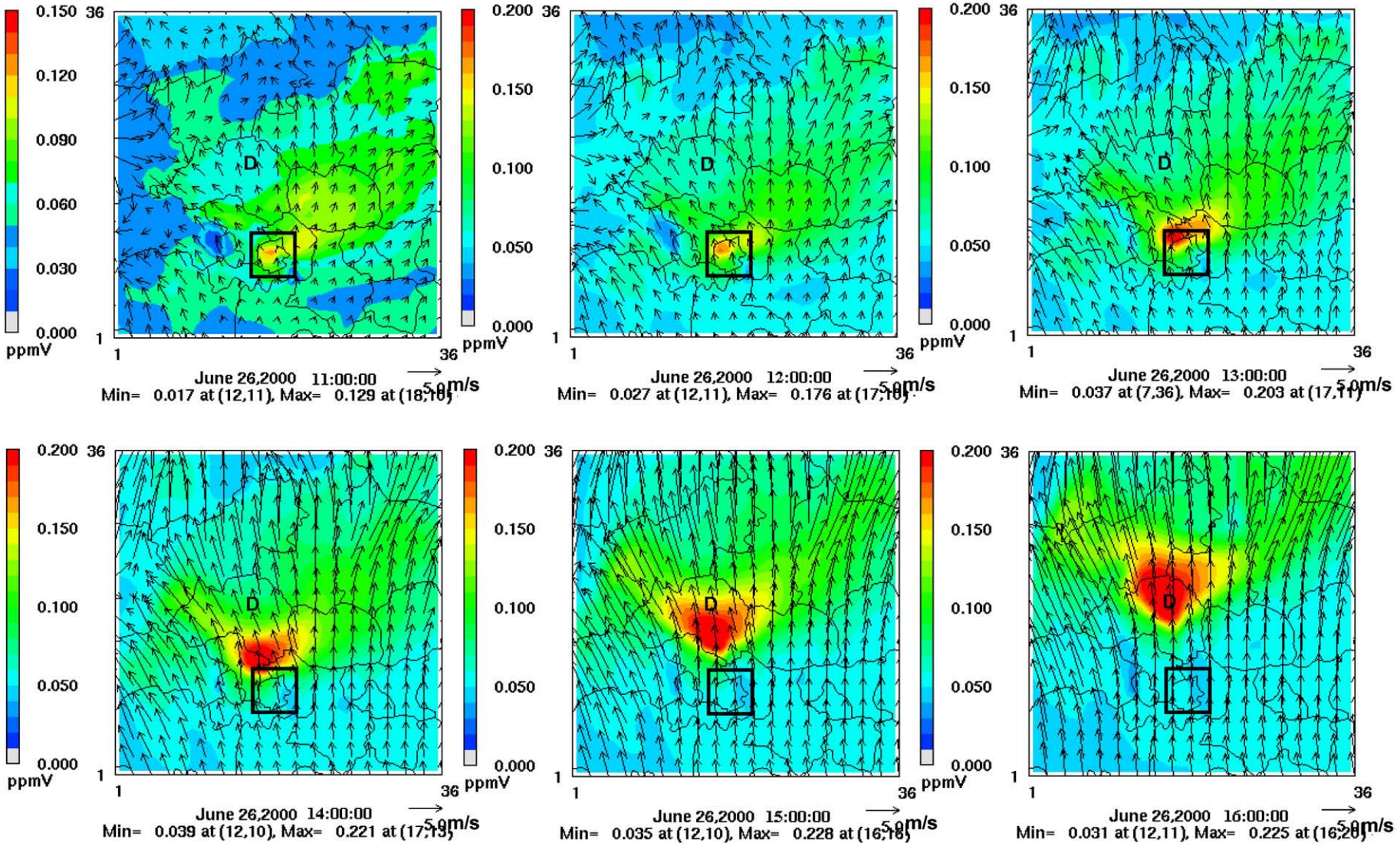

Fig. 4 – Simulated O_3 evolution in the surface layer of the Beijing area during 1100–1600 LST on 26 June 2000; inner box defined the urban area, letter 'D' in the figure denotes Dingling.

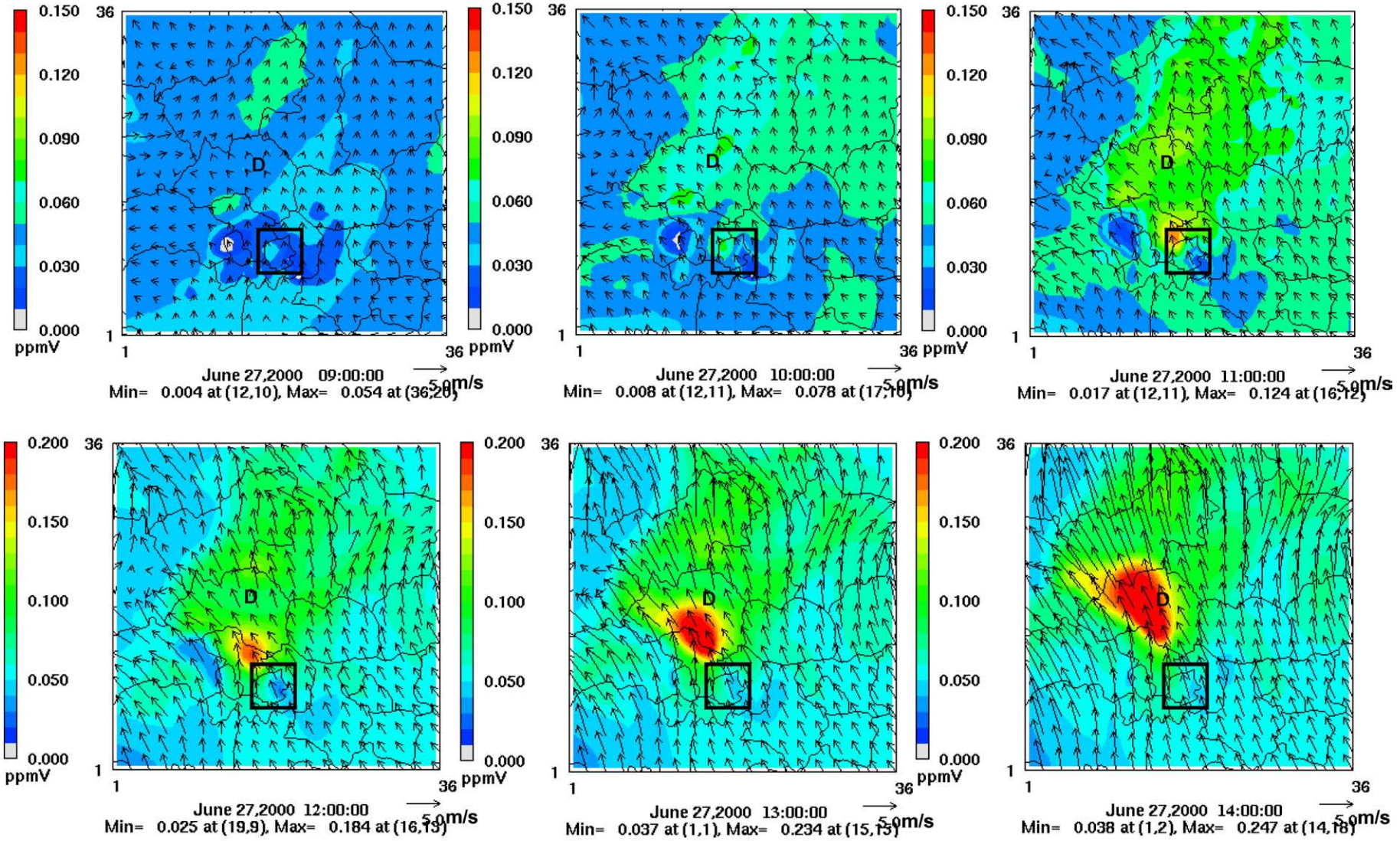

Fig. 5 – Simulated O_3 evolution in the surface layer of the Beijing area during 0900–1400 LST on 27 June 2000.

the urban and suburban areas, with a horizontal resolution of 4 km. Fourteen layers were unequally spaced from the ground to approximately 10 km altitude, with 9 layers located under 1 km to resolve the boundary layer process. The height of the lowest layer is about 20 m. The simulation period was from 24 June to 3 July 2000.

The meteorology field was derived from the MM5 simulation. To shift the simulated meteorology variables close to observed values, a 4-dimensional assimilation was performed using rawinsonde data and hourly meteorology observations from ground stations in urban and suburban areas of Beijing.

The 1×1° anthropogenic emission inventory (Streets et al., 2003) maintained by CGRER (Center for Global and Regional Environmental Research) at the University of Iowa was used for the East Asia simulation (first-level domain). Biogenic VOC emissions were obtained from the GEIA (Global Emissions Inventory Activity) monthly global inventory (Guenther et al., 1995). SMOKE (Sparse Matrix Operator Kernel Emissions System: www.cmascenter.org/html/models.html) converted the various types of emission data to files with the format required by CMAQ.

The emission inventory at the second- and third-level nesting domain (Beijing area) was constructed based on the emission survey in North China for the year 2000 (Wang, 2002; Wang and Li, 2003), while the emission inventory for the Beijing urban and suburban area was prepared by the Beijing Environmental Science Institute. The basic data used for emission estimates included annual emission data from a variety sources reported by the local Environment Protection Bureau, as well as statistical data on energy, environmental protection, social and economic factors, etc., derived from year books published in the areas of concern. The species included NO_x, VOCs, CO, SO_2, PM_{10}, and NH_3. The VOC inventory was compiled by sector, including mobile sources, the transportation and marketing of petroleum products, solvent utilization, industrial processes, and stationary source combustion, etc. For the two nested domains, the GEIA biogenic VOC emission inventory was used to determine emissions from vegetation.

3.1. *Simulated evolution of O_3 concentrations*

Figs. 4 and 5 show the evolution of simulated O_3 concentrations over the Beijing area on 26 and 27 June, 2000, respectively. In the morning hours of 26 June, when the wind field was in transition, wind speed was low and conditions were mostly calm wind in the urban area. This facilitated the development of local photochemistry, leading to a large accumulation of O_3. At 1200 LST, high O_3 concentrations developed first within the urban area, with peak values located close to the urban center. During 1300–1400 LST on 26 June, the area of high O_3 concentrations moved to the northern part of the urban area, covering the Olympic Center and Peking University with higher peak values than those at 1200 LST. After 1400 LST, a strong southerly wind prevailed over the whole domain, transporting O_3 to the downwind area. During propagation of the urban plume, O_3 concentrations showed an increasing trend, indicating that O_3 precursors in the urban plume produced O_3 continuously via photochemistry, thus giving rise to the higher O_3 peak in the downwind area than that in the urban area. For 27 June, the simulated O_3 evolution differed from that for 26 June. Because transportation upon the strong southerly wind began earlier than that on the previous day, high O_3 concentrations appeared first in the downwind area rather than the urban area, again showing an increasing trend with propagation of the urban plume. The simulated evolution of O_3 concentrations for 26 and 27 June generally corresponds with the observation evolution described in Section 2.2. Accordingly, we conclude that the model simulation provides a sound representation of the typical summertime O_3 formation process over the Beijing area.

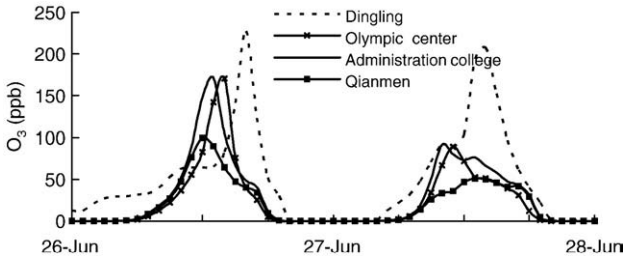

Fig. 6 – Simulated diurnal variations in O_3 at specific sites in the urban area and the downwind area of Dingling during 26 and 27 June 2000.

Fig. 6 shows the simulated diurnal variations in O_3 at selected urban locations and the downwind area of Dingling over the days of 26 and 27 June. The simulated O_3 peak values and pattern of variation are generally in good agreement with observed data. The observed O_3 peak at Dingling appeared 2–3 h later than that in the urban area; this delay was also well represented by the simulation.

4. Process analysis of O_3 formation

4.1. *Contribution analysis*

IPR equipped in CMAQ was used to isolate the contribution of each process to variations in O_3. Fig. 7a and b shows diurnal variations in the contributions of physical or chemical process to O_3 formation at Dingling from 26 to 27 June at surface layer and 500 m height respectively, as calculated using IPR. In the morning hours of 26 June, O_3 levels produced by local photochemistry were rather low, around 60–70 ppb. It was only after the arrival of the high-O_3 urban plume at Dingling in the afternoon that O_3 levels increased, approaching 200 ppb. During the period, O_3 increase by horizontal transportation was stronger at 500 m height than that at the surface layer, making a strong vertical O_3 transportation from upper level to the surface layer, whereas, the effects were rather weak for the other hours. An analysis of O_3 formation for the urban atmosphere shows that upper level of the boundary layer produced O_3 much higher than that at the surface layer, and the vertical O_3 transportation from upper level is a major mechanism of O_3 increase at the surface layer (Xu and Zhangm, 2006a). This indicates that the strong vertical O_3 import at Dingling surface layer is aroused by the urban plume arrival. On 27 June, local O_3 production was much higher than that on 26 June, and high O_3 input by transportation occurred

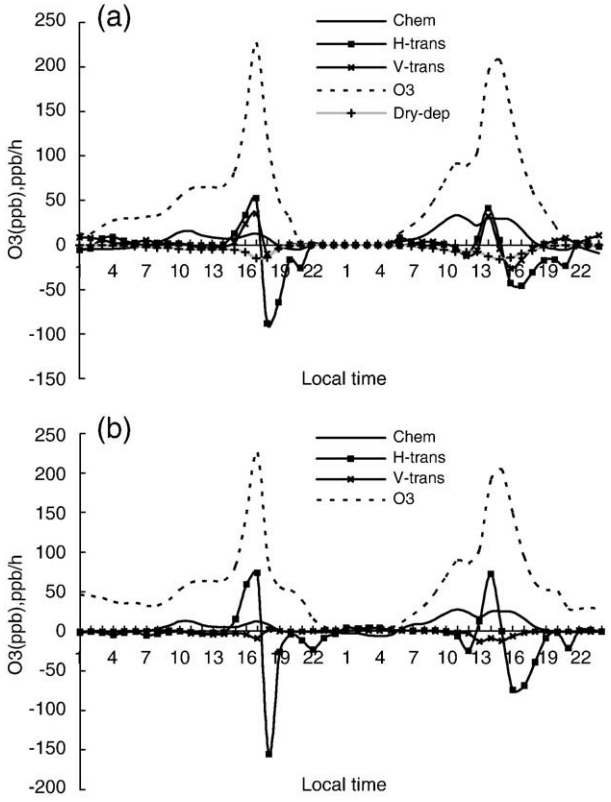

Fig. 7 – Contributions of different processes to O_3 formation at (a) the surface layer and (b) 500 m height at Dingling during 26 and 27 June 2000, where O_3 denotes O_3 concentrations, Chem denotes O_3 produced by photochemistry, Dry-dep denotes O_3 loss by dry deposition, H-trans and V-trans denotes O_3 increase by horizontal and vertical transportation respectively.

later in the afternoon, arising from well-developed photochemistry in the urban plume, thereby further enhancing the O_3 concentrations at Dingling and leading to another high-O_3 episode.

Although the magnitudes of O_3 increase from 0800 LST to the hour of peak O_3 were similar on both 26 and 27 June, as shown in Fig. 8, the major contributors to O_3 increase differed on the two days. On 26 June, direct O_3 input via the arrival of the urban plume was much higher than that on 27 June, being the largest contributor to the recorded O_3 increase. In contrast, on 27 June the local O_3 production was much higher than that on 26 June, surpassing direct O_3 input in becoming the major contributor to the recorded O_3 increase.

The low levels of emissions around Dingling mean that only minor O_3 is produced by local photochemistry. The process analysis revealed that the high O_3 levels recorded at Dingling may result from two types of mechanism. First, in the case that transportation began late in the afternoon, O_3 precursors accumulated at the urban area during the morning hours, meaning that photochemistry was influential at this site. Once the strong transportation began, O_3 increased continuously in the urban plume with ongoing propagation. Finally, when the plume arrived at Dingling, high O_3 concentrations were recorded, making direct O_3 input via transportation the major contributor to the O_3 increase. Second, in the case that strong transportation started early in the day, O_3 precursors were transported rapidly to the downwind area, even in the morning hours. This led to increasing local photochemistry at Dingling, thereby making local O_3 production the major contributor to the recorded O_3 increase.

4.2. *O_3 production on 26 and 27 June*

In order to further explore the diurnal variations of O_3 production, we use IPR and IRR to quantify the important chemical and physical processes related to O_3 formation from 26 to 27 June at Dingling. As shown in Fig. 9, $NO \rightarrow NO_2$ conversion by radicals showed two daytime peaks on each day, corresponding to peaks in O_3 production by photochemistry. The first peak arose from typical local photochemistry. In the morning, as atmospheric activity increased gradually with intensifying photolysis, $NO \rightarrow NO_2$ conversion and O_3 produced chemically reached a peak close to midday. In the afternoon, as high O_3 concentrations arrived with the approaching urban plume, the decreasing trend in the creation of new radicals began to increase again, reaching a second peak. This led to an increase in atmospheric activity, resulting in another peak in $NO \rightarrow NO_2$ conversion in the afternoon.

At Dingling, many differences were recorded in the photochemistry of O_3 production between 26 and 27 June. In the morning hours of 26 June, before the start of transportation of

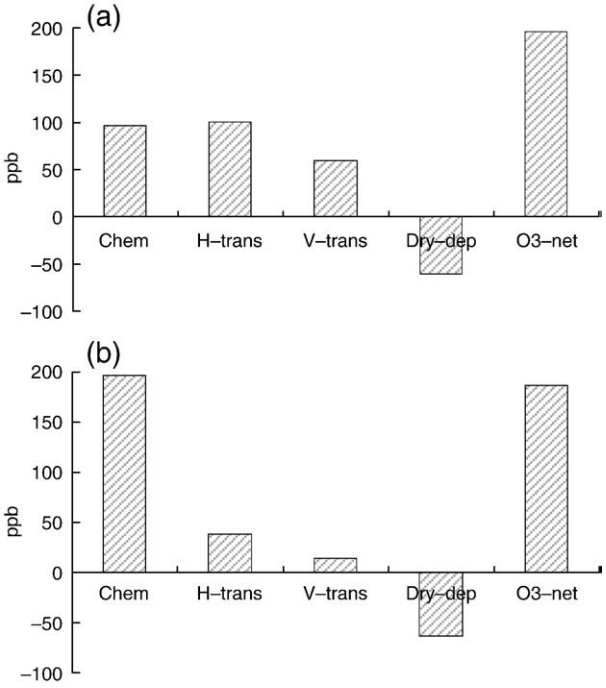

Fig. 8 – Contributions of different processes to O_3 increase from 0800 LST to peak hours at Dingling on (a) 26 June and (b) 27 June 2000, where O_3-net is the net O_3 increase obtained by summing the contributions from photochemistry (Chem), horizontal transportation (H-trans), vertical transportation (V-trans), and Dry deposition (Dry-dep) processes.

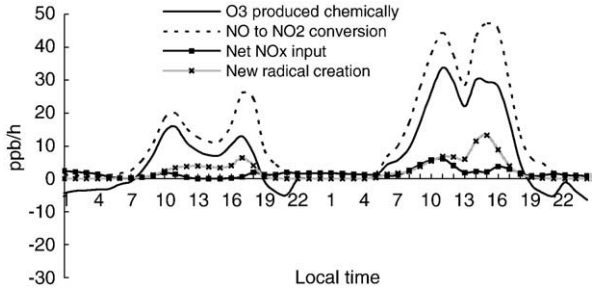

Fig. 9 – Diurnal variations in processes related to chemical O_3 production at Dingling from 26 to 27 June 2000, where 'Net NO_x input' is the sum of local NO_x emission and NO_x input by transportation.

the urban plume, photochemistry at Dingling was mainly controlled by local emissions, meaning that atmospheric activity was low, with low rates of $NO \rightarrow NO_2$ conversion and O_3 production. On 27 June, when strong transportation of the urban plume began early in the day, photochemistry at Dingling was affected by the urban plume even during the morning hours. Net NO_x input and the creation of new radicals exceeded the rates recorded on 26 June, leading to high atmospheric activity in which $NO \rightarrow NO_2$ conversion and the amount of O_3 produced locally were higher than those on 26 June.

5. Comparison of radical cycles

Radicals are the most active species in the atmospheric photochemical system, and the OH, RO_2, and HO_2 radicals play an important role in O_3 formation. With the photolysis of O_3, aldehydes, HONO, and other species, new OH, RO_2, and HO_2 radicals are created and enter the radical cycle (Bowman and Seinfeld, 1994). The more new radicals created, the higher the atmospheric activity. In the radical cycle, transfer among RO_2, HO_2, and OH radicals oxidizes VOC and converts NO to NO_2, thereby accomplishing the major oxidation processes involved in O_3 formation. Finally, the radicals are eliminated by the termination paths of the RO_2, HO_2, and OH radicals, due to the formation of HNO_3, PAN, and H_2O_2, etc.

Such a radical cycle (see Fig. 10) can reveal the characteristics of the origins of new radicals, the efficiency of the radical cycle, atmospheric activity, and the NO_x or VOC control regime of O_3 formation at specific locations. All items in the radical cycle can be calculated using the IRR module in CMAQ. Here, a typical period of O_3 formation, 0800–1600 LST, was selected for a comparison of radical cycles, to further explore the differences in the photochemical characteristics of O_3 formation in the urban area and its downwind area, or at a given site under different meteorological conditions.

5.1. *Comparison of urban area and downwind area*

Fig. 10 provides a comparison of the radical cycle for the urban area and its downwind area, Dingling, for the period 0800–1600 LST on 26 June. Given that obvious transportation occurred only after 1500 LST on 26 June, photochemistry during this period likely represents the characteristics of local emissions. For the two locations, large differences existed in the radical cycles in terms of the creation of new radicals, cycling speed, and radical termination paths.

On 26 June, the total amount of new radical creation at Dingling was 27 ppb, much lower than the 64 ppb recorded in the urban area. At Dingling, where O_3 photolysis was the major source, 48% of new radicals originated from the creation of new OH. In the urban area, 69% of new radicals originated from the RO_2 and HO_2 creation paths, with much higher amounts being produced than at Dingling. As the peroxide radicals were mainly produced via the photolysis of formaldehyde and other intermediates created by oxidized VOC, the high rates of VOC emission in the urban area may have led to the high rates of HO_2 and RO_2 formation.

In terms of the creation of OH radicals, the amount at Dingling was 7 ppb lower than that in the urban area, reflecting the difference in HONO photolysis between the two locations. In the urban area, high NO_x and PM_{10} concentrations facilitated the NO_2 heterogeneous reaction of $NO_2 \xrightarrow{PM} 0.5HONO + 0.5HNO_3$ (Xu and Zhang, 2006b), in which HONO is one of the products. Low NO_x and PM_{10} concentrations limited the extent of the NO_2 heterogeneous reaction at Dingling. In CMAQ-MADRID, the reaction probability γ is introduced to account for the heterogeneous reaction, which convolve processes of mass accommodation into the liquid phase, diffusion within the liquid phase, and chemical reaction. For NO_2 heterogeneous reaction, γ_{NO_2} has a range of 10^{-6}–10^{-3} in results of laboratory experiments. We also do test runs to detect the effects at each of the low and high bound of the range. Results show that OH produced by NO_2 heterogeneous reaction is quite sensitive to the γ_{NO_2} value. In the urban area, OH produced by NO_2 heterogeneous reaction during the same period is much less than 1 ppb at the low bound, whereas the value reaches 86 ppb at the high bound. In the control run, the value is 7 ppb. As we know that γ is quite uncertain for each heterogeneous reaction, O_3 model including such processes is just at a tentative stage now. But, the processes maybe important in China, as the air have a high

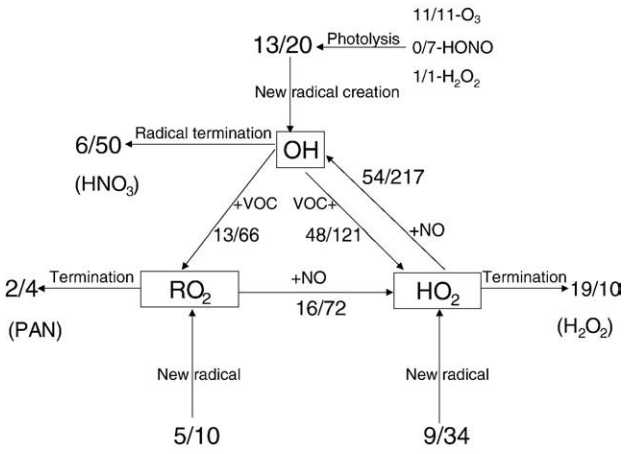

Fig. 10 – Comparison of radical cycles for Dingling and the urban area during 0800–1600 LST on 26 June (each pair of numbers denotes the results obtained for Dingling and the urban area; unit: ppb).

aerosol loading circumstances. In CMAQ control run, γ_{NO_2} is taken a value of 10^{-4}, which is suggested by Jacob (2000) based on a comprehensive consideration of lab results on NO_2 uptake by aqueous solutions and field studies. In the Beijing area, as the relative humidity is high in summer, it is appropriate to use the parameter of moist aerosol in the simulation.

In the radical cycle, the more conversion among radicals, the more VOC oxidation and NO→NO_2 conversion occurs, resulting in high atmospheric activity. In comparing radical conversion for the urban area and Dingling, it was found that conversion was relatively slow at Dingling, about 25% of the rate for the urban area. The length of the radical cycle, L_{OH}, as prescribed by Seinfeld and Pandis (1998), is the average number of times that a newly created radical propagates through the radical cycle before its termination. We calculated this value in terms of cycles (i.e., 3.0 and 4.4) for Dingling and the urban area, respectively. The longer the length of the radical cycle, the longer that radicals stay in the atmosphere, leading to a efficiency for the radical cycle and high concentrations in the urban area.

In assessing radical termination by each pathway in the urban area, we found that about 78% of radicals were eliminated via the OH termination path, with HNO_3 being the major product. This finding indicates that although VOC emissions were high in the urban area, NO_x was still in surplus, and O_3 formation occurred in a VOC-limited regime. At Dingling, the major termination path was different from that in the urban area, with about 70% of radicals eliminated via the HO_2 termination path, making H_2O_2 the major product. The low rate of NO_x emission at Dingling meant that only small amounts of radicals were terminated via the reaction $NO_2+OH \rightarrow HNO_3$. As insufficient NO_2 reacted with radicals to initiate termination, termination between radicals became an important path. In this case, when more NO_x are added, more radicals will continue in the cycle than by the termination path between radicals. Thus more NO→NO_2 conversion occurred, leading to more O_3 production. So, the regime of O_3 formation determined by local emissions changed to a NO_x-limited case at Dingling.

Sillman (1995) proposed the ratio P_{H_2O2}/P_{HNO_3} to identify the NO_x or VOC regime for O_3 formation, where P_{H_2O2} and P_{HNO_3} are the production rates for H_2O_2 and HNO_3, respectively, with a transition ratio of 0.35. Given that the major products of the OH and HO_2 termination paths are HNO_3 and H_2O_2, respectively, P_{H_2O2}/P_{HNO_3} can be estimated from the values of HO_2 and OH termination in the radical cycle. In the urban area, the calculated ratio is 0.1, lower than the transition ratio. This finding provides further evidence that the urban area was subjected to a VOC-limited regime of O_3 formation. The ratio at Dingling was 1.58, much higher than the transition value, demonstrating that Dingling was subjected to a NO_x-limited regime determined by local emissions.

5.2. *26 June and 27 June*

Fig. 11 compares the radical cycle for 26 and 27 June at Dingling during the period 0800–1600 LST. On 27 June, the radical cycle was apparently affected by intrusion of the urban plume. The rapid approach of the urban plume on 27 June meant that new

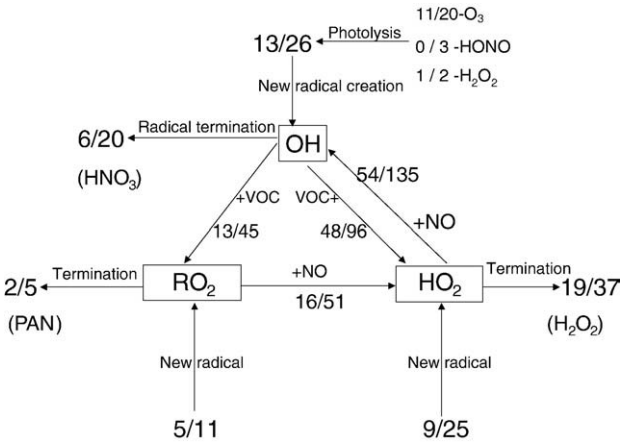

Fig. 11 – Comparison of radical cycles for 26 and 27 June 2000 at Dingling during 0800–1600 LST (each pair of numbers denotes the results for 26 and 27 June; unit: ppb).

radical creation increased from 27 ppb on 26 June to 62 ppb on 27 June; the dominant path of new radical creation also changed. On 27 June, a larger amount and higher percentage of new radical creation was derived from the RO_2 and HO_2 creation paths, possessing the characteristics of the photochemistry of the urban plume. On 27 June, 3 ppb of new OH radical arose from HONO photolysis, which resulted from the NO_2 heterogeneous reaction in the urban atmosphere; the value was well below 1 ppb on 26 June.

The low level of emissions at Dingling meant that the early arrival of the urban plume on 27 June led to increased atmospheric activity, leading in turn to remarkably high levels of conversion among radicals. As shown in Fig. 11, the conversion values increased by at least a factor of 2 compared with those on 26 June, and the length of radical cycle increased from 3.0 on 26 June to 3.2 on 27 June.

The radical termination paths also showed clear changes on the two days. On 26 June, 70% of radicals were eliminated via the HO_2 termination path. This Figure decreased to 59% on 27 June, with more radicals being eliminated via the OH termination path. The estimated value of P_{H_2O2}/P_{HNO_3} decreased from 1.58 on 26 June to 0.84 on 27 June, implying that the regime of O_3 formation at Dingling changed to some extent with the intrusion of the urban plume on 27 June.

6. Conclusion

Typical summertime high-ozone episodes in the Beijing area were identified via analyses of wind fields and the monitoring of pollutants. The representative processes were well reproduced by the 3-dimensional air-quality model CMAQ-MADRID. Process analysis in the model run revealed large differences in O_3-forming photochemistry between the urban area and its downwind area. The urban area existed in a VOC-limited regime of O_3 formation, while the urban downwind area changed gradually to a NO_x-limited condition. The urban downwind area, Dingling, is readily affected by intrusion of the urban plume. Detailed process analysis indicated that although the O_3 peaks reached the same level on 26 and 27 June

2000, the dominant process contributing to the O_3 increase was different on each day. On 26 June, the major contributor to the O_3 peak at Dingling was the arrival of high O_3 with the urban plume; in contrast, on 27 June O_3 precursors were transported rapidly to the urban downwind area, resulting in O_3 production by local photochemistry becoming the major contributor to the high-O_3 episode.

This study does not only reproduce the observed high O_3 concentrations, but also depicts the evolution of pollution based on an accurate account of the processes. It is suggested that the accuracy of the model simulation needs to be further tested using additional observations, such as measurements of radical concentrations, the vertical O_3 profile, precursors, and some intermediates of photochemistry in the boundary layer, as well as diurnal variations. The compilation of the emission inventory, as a key element of the modeling, is always a difficult task, especially in China given its rapid economic development. The emission inventory therefore requires additional investigation. Only once the simulation is able to accurately represent the chemical and physical processes that actually happened should the results of further process analysis or scenario simulations for various control strategies be viewed as feasible results.

Acknowledgments

This work was supported by Hi-Tech Research and Development Program of China-2006AA06A306, and China National Basic Research and Development Program 2002CB410801 and 2002CB211600. Authors would like to thank anonymous referees for valuable comments which helped to improve this manuscript.

Appendix A. Supplementary data

Supplementary data associated with this article can be found, in the online version, at doi:10.1016/j.scitotenv.2008.02.013.

REFERENCES

Bowman FM, Seinfeld JH. Ozone productivity of atmospheric organics. J Geophys Res 1994;99:5309–24.

Byun DW, Ching JKS, editors. Science algorithms of the EPA Models-3 community multi-scale air quality (CMAQ) modeling system. *Rep. EPA-600/R-99/030*. Research Triangle Park, N.C.: National Exposure Research Laboratory; 1999. Chapter 1, 18 pp.

Cai XH, Guo Y, Liu HZ, Chen JY. Flow patterns of lower atmosphere over Beijing area. Acta Scientiarum Naturalium Universitatis Pekinensis 2002;vol.38(3):387–92 (in Chinese).

Climatology Dataset Division of Beijing Meteorology Agency. Climatology in Beijing. Beijing: Peking press; 1987. p. 69–77. (in Chinese).

Gery MW, Whitten GZ, Killus JP, Dodge MC. A photochemical kinetics mechanism for urban and regional scale computer modeling. J Geophys Res 1989;94:12,925–56.

Grell GA, Dudhia J, Stanffer DR. A description of the Fifth-generation Penn State/NCAR Mesoscale Model (MM5). NCAR Tech. Note, NCAR/TN-398+STR; 1994. 138 pp.

Guenther A, et al. A global model of natural volatile organic compound emissions. J Geophys Res 1995;100:8873–92.

Huang Jian-Ping, Fung Jimmy CH, Lau Alexis KH, Qin Yu. Numerical simulation and process analysis of typhoon-related ozone episodes in Hong Kong. J Geophys Res 2005;110(D5) CiteID D05301.

Jacob D. Heterogeneous chemistry and tropospheric ozone. Atmos Environ 2000;34:2132–59.

Jeffries HE, Tonnesen S. A comparison of two photochemical reaction mechanisms using mass balance and process analysis. Atmos Environ 1994;28(18):2991–3003.

Li YY, Qu SH, Zhou MY. Wind field analysis in the Beijing area. Acta Scientiae Circumstantise 1982;2(4):351–7 (in Chinese).

Nenes A, Pandis SN, Pilinis C. ISORROPIA: a new thermodynamic model for inorganic multicomponent atmospheric aerosols. Aquat Geochem 1998;4:123–52.

Seinfeld JH, Pandis SN. Atmospheric chemistry and physics from air pollution to climate change. John Wiley & Sons, Inc.; 1998. p. 308–9.

Shao M, Tang XY, Zhang YH, Li Wenjun. City cluster in China: air and surface water pollution. Front Ecol Environ 2006;4(7):353–61.

Sillman S. The use of NO_Y, H_2O_2, and HNO_3 as indicators for ozone-NO_x-hydrocarbon sensitivity in urban locations. J Geophys Res 1995;100(D7):14175–88.

Steve CS, Jiang Weimin, Yin Dazhong, Roth Helmut, Giroux Eric. Evaluation of CMAQ O3 and PM2.5 performance using Pacific 2001 measurement data. Atmos Environ 2006;40(26):2735–49.

Streets DG, et al. An inventory of gaseous and primary aerosol emissions in Asia in the year 2000. J Geophys Res 2003;108 (D21):8809. doi:10.1029/2002JD003093.

Streets DG, et al. Air quality during the 2008 Beijing Olympic Games. Atmos Environ 2007;41(3):480–92.

Wang X. A numerical simulation study on ozone and secondary aerosol in Regional atmosphere, Ph.D dissertation, College of Environmental Sciences, Peking University, Beijing. 2002, (in Chinese).

Wang X, Li J. A case study of ozone source apportionment in Beijing. Acta Scientiarum Naturalium, Universitatis Pekinensis 2003;39(2):244–53 (in Chinese).

Wang Zifa, Li Jie, Wang Xiquan, Pochanart Pakpong, Akimoto Hajime. Modeling of regional high ozone episode observed at two mountain sites (Mt. Tai and Huang) in East China. J Atmos Chem 2006;55(3) November.

Xu J, Zhang YH. Process analysis of O_3 formation in summer at the Beijing urban area[J]. Acta Scientiae Circumstantise 2006a;26 (6):973–80 (in Chinese).

Xu J, Zhang YH. Numerical study for the impacts of heterogeneous reactions on Ozone formation in Beijing urban area. Adv Atmos Sci 2006b;23(4):605–14.

Xu M, Jiang WM, Ji CP, Liu HT, Gao YH, Wang XY. Numerical modeling and verification of structures of the boundary layer over Beijing area. J Appl Meteoro Sci 2002;13:61–8 Suppl. January, (in Chinese).

Zhang Yuanhang, Shao Kesheng, Tang Xiaoyan, Li Jinlong. The study of urban photochemical smog pollution in China. Acta Scientiarum Naturalium Universitatis Pekinensis 1998;34 (2–1):392–400 (in Chinese).

Zhang Meigen, Uno Itsushi, Zhang Renjian, Han Zhiwei, Wang Zifa, Pu Yifen. Evaluation of the Models-3 Community Multi-scale Air Quality (CMAQ) modeling system with observations obtained during the TRACE-P experiment: comparison of ozone and its related species. Atmos. Environ. 2006;40(26):4874–82.

Zhang Y, et al. Development and application of the Model of Aerosol Dynamics, Reaction, Ionization and Dissolution (MADRID). J. Geophys. Res. 2004;109:D01202. doi:10.1029/2003JD003501.